www.czasopisma.pan.pl PAN www.journals.pan.pl

ARCHIVES of FOUNDRY ENGINEERING

ISSN (2299-2944)
Volume 2020
Issue 3/2020

112 – 118

10.24425/afe.2020.133339

19/3

Published quarterly as the organ of the Foundry Commission of the Polish Academy of Sciences

Fabrication Optimization of Al 7075/Expanded Glass Syntactic Foam by Cold Chamber Die Casting

C. Bolat *, A. Goksenli
Istanbul Technical University, Faculty of Mechanical Engineering, 34437, Istanbul, Turkey
* Corresponding author. e-mail address: caginbolat@itu.edu.tr

Received 08.05.2020; accepted in revised form 13.07.2020

Abstract

Recently, aluminum matrix syntactic foams (AMSFs) have become notably attractive for many different industrial areas like automotive, aerospace, construction and defense. Owing to their low density, good compression response and perfect energy absorption capacity, these advanced composite materials are also considered as strong alternatives to traditional particle reinforced composites and metal foams. This paper presents a promising probability of AMSF fabrication by means of industrial cold chamber die casting method. In this investigation, contrary to other literature studies restricted in laboratory scale, fully equipped custom-build cold chamber die casting machine was used first time and all fabrication steps were designed just as carried out in the real industrial high pressure casting applications. Main casting parameters (casting temperature, injection pressure, piston speed, filler pre-temperature and piston waiting time) were optimized in order to obtain flawless AMSF samples. The density alterations of the syntactic foams were analyzed depending upon increasing process values of injection pressure, piston speed and piston waiting time. In addition, macroscopic and microscopic investigations were performed to comprehend physical properties of fabricated foams. All these efforts showed almost perfect infiltration between filler particles at the optimized injection parameters.

Keywords: Syntactic foams, Aluminium alloys, Expanded glass, Cold chamber die casting, Process optimization

1. Introduction

Aluminum matrix syntactic foams (AMSFs) are advanced engineering materials comprising of an Al alloy matrix and porous ceramic or metallic filler material [1-3]. The most remarkable feature of these materials is that they can behave like both particle reinforced composites and conventional closed cell metal foams. In recent years, because of their perfect energy absorption capacity, high compression strength, low density and good tribological properties, AMSFs have become popular for several industrial areas such as automotive, aerospace, construction and defense [4-5]. Thanks to highly hard and porous (or hollow) filler particles distributed in the Al matrix, AMSFs display better mechanical properties than traditional Al foams. In the technical literature, most of researches have utilized different types of filler materials such as fly ash cenospheres, hollow ceramic spheres, glass balloons and hollow metal spheres [3-6]. Moreover, in some studies, because widely used engineered hollow ceramic fillers are relatively expensive due to their sophisticated production techniques, volcanic rock based expanded perlite, expanded glass and pumice particles have been tried to use as filler materials [2-7,8].

Even though detailed casting features of conventional particle reinforced Al matrix composites have been examined for many years [9-11], efforts on AMSFs have performed usually on their mechanical properties. AMSFs are typically manufactured by

infiltration casting or stirring technique. Each method has its own advantages and limitations in terms of ease of implementation and total cost. While the infiltration casting provides homogenous and controllable foam structure, the stirring technique is low cost and easily applicable. If the infiltration casting methods are looked at briefly, it is obvious that gravity assisted (onward) pressure infiltration, counter gravity (backward) infiltration and gas/vacuum assisted pressure infiltration are the most preferred methods by many researchers. For instance, Zhang et al. and Tao et al. used gravity assisted infiltration in their works and they fabricated commercially pure Al(cp-Al)/fly ash cenosphere and Al 6082/ceramic microsphere syntactic foams respectively [12-13]. In other surveys, Taherishargh et al. introduced novel volcanic rock based fillers like expanded perlite and pumice for Al A356 matrix syntactic foams by applying counter gravity infiltration [2, 7]. Similarly, Fiedler et al. used counter gravity infiltration to scrutinize effects of the particle size on the mechanical properties of expanded glass filled A356 syntactic foams [8]. On the other hand, Orbulov et al. showed that gas/vacuum pressure infiltration methods also were effective for AMSF fabrication [6, 14]. In their recent study, the same research group analyzed low frequency damping behavior of cp-Al and AlSi12 syntactic foams fabricated with gas pressure infiltration [15]. Aside from the infiltration casting method, stirring technique is also used for syntactic fabrication even though it may cause nonhomogeneous filler distribution owing to density mismatch between matrix and filler material. Herein, Goel et al. focused on high strain rate deformation behavior of fly ash cenosphere filled Al 2014 syntactic foam and utilized stir mixing method in the fabrication stage [16]. Mondal et al. compared microstructural and compression characteristics of alumina and fly ash cenosphere reinforced Al 2014 syntactic foam made through stir mixing [17]. Besides, Mondal et al tried the same blending technique in order to comprehend effect of fly ash cenosphere size on the dry sliding wear behavior of LM13 syntactic foam [18]. Lately, some promising powder metallurgical methods have also been examined on the purpose of creating an alternative to the two main fabrication ways (infiltration and stirring) [19].

In this paper, our aim was to fabricate AMSFs first time by means of fully automated and industrial focused cold chamber die casting rather than widely used laboratory scale methods. In addition, all process parameters were optimized to obtain high quality products with different filler size and physical properties of foam samples were examined elaborately by performing macro and micro investigations.

2. Materials and Method

2.1. Materials

In this study, heat treatable series of Al 7075 alloy was preferred as matrix material due to its good ductility, high strength, sufficient toughness, corrosion resistance and widespread usage in major sectors like automotive, aerospace, defense and construction. Its chemical composition was 5.68 wt. % Zn, 2.39 wt. % Mg, 1.4 wt. % Cu, 0.21 wt. % Fe, 0.2 wt. % Si, 0.18 wt. % Mn and 0.034 wt. % Ti.

As for porous filler particles, recycled expanded glass (EG) spheres supplied from Omnis Composite Limited Company were used. Owing to its unique porous structure, EG particles (73 wt. % SiO_2, 14 wt. % Na_2O, 8 wt. % CaO, 4 wt. % MgO, 0.15 wt. % Al_2O_3 and 0.1 wt. % Fe_2O_3) have low bulk density (0.2 – 0.35 g/cm^3), low thermal conductivity (0.065 W/mK) and perfect acoustic features. Also, if it is considered that majority of the syntactic studies have focused on expensive engineered hollow ceramic fillers, these cheap and rarely utilized porous glass granules can be serious alternatives for the upcoming investigations. Fig.1 given below shows macroscopic and microscopic images of the EG spheres having different size range.

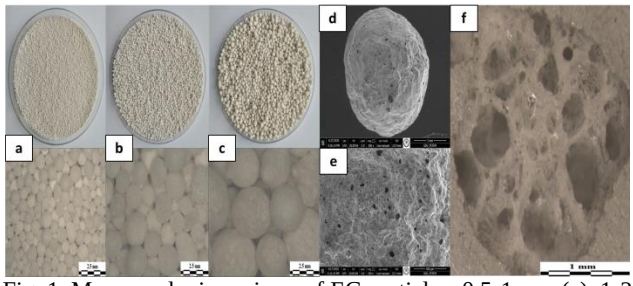

Fig. 1. Macro and micro views of EG particles; 0.5-1 mm (a), 1-2 mm (b), 2-4 mm (c), SEM images (d, e) and inner porous structure (f)

2.2 Method

On the purpose of rapid and industry focused fabrication, contrary to frequently applied laboratory scaled infiltration techniques, fully equipped custom build automatic cold chamber die casting method was used. Fig. 2 indicates both real image of the casting machine and schematic view of the process in detail.

If the process is describe briefly, at first the machine was switched on and all sensors were activated. Then, two pieced die and sprue were preheated up to approximately 300°C to provide unproblematic liquid alloy flow. For melting of cylindrical Al 7075 blocks and preheating of porous EG spheres, an induction furnace (max. 1100°C capacity) and an electrical resistance furnace (max. 1100°C capacity) were used respectively. Following the melting of Al matrix, preheated EG spheres were placed into the preheated die cavity and the die was completely sealed with two pins and four bolts. When all sensors were controlled and protective outer caps were closed down, molten and dross removed Al alloy in a graphite ladle was poured into the sprue. Immediately after that, in order to get flawless filtration between EG particles, process pressure was applied with an automatized injection piston. All process parameters (piston speed, pressure and waiting time) were controlled with special sensors during the operation. Although the injection piston reached the end point of the sprue line in every process, it was waited for a while (10-30 sec.) at pressure active position because of the possibility of better infiltration even in very narrow gaps. Finally, the die was opened up automatically and fabricated foam sample having 60 mm diameter and 80 mm length was removed from the die cavity.

In the end, thanks to the fully equipped cold chamber die casting, nine different cylindrical foams with 60 mm diameter and 80 mm length were produced without any setbacks. Density values of the fabricated foams were found by dividing sample mass values to their cylindrical volumes and these values altered between 1.82 and 2.06 g/cm^3.

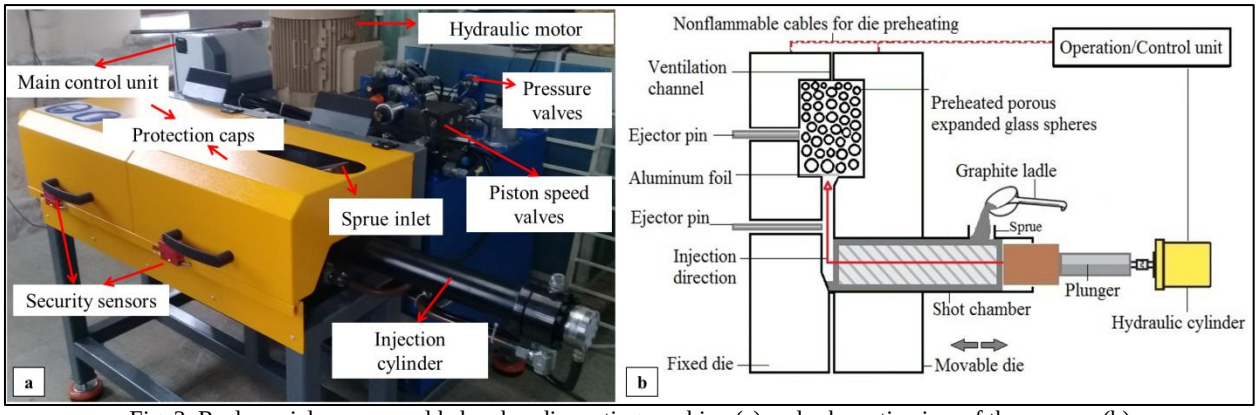

Fig. 2. Real special purpose cold chamber die casting machine (a) and schematic view of the process (b)

3. Experimental Studies

3.1 Optimization of Process Parameters

With the intention of increasing product diversity, three different filler materials having 0.5-1, 1-2 and 2-4 mm diameter were used in the Al matrix and nine different samples were fabricated for further analysis. Herein, firstly, main process parameters shared in Table 1 were optimized for medium size (1-2 mm) filler reinforced syntactic foams so that, in the light of that approach, the same work could be performed easily for small and big size fillers. Besides, all fabricated samples were inspected carefully in terms of infiltration sensitivity and Fig.3 shows fabrication development step by step depending on casting variables.

Table 1.
Main process parameters for medium size EG filled syntactic foams

Process No	Casting Temperature (°C)	Injection Pressure (bar)	Piston Speed (mm/sec)	Filler Preheat Temperature (°C)	Piston Waiting Time (sec)
P1	680	170	20	400	10
P2	700	170	20	400	10
P3	700	170	20	500	10
P4	700	200	30	500	20
P5	700	200	30	550	20
P6	730	170	20	400	10
P7	730	170	20	500	10
P8	730	170	20	550	10
P9	730	200	30	500	20
P10	730	200	30	550	20

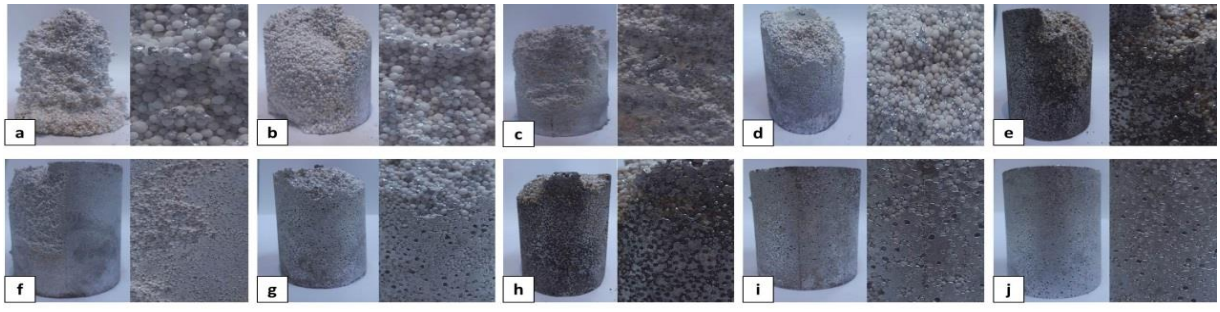

Fig. 3. Product development steps : P1(a), P2(b), P3(c), P4(d), P5(e), P6(f), P7(g), P8(h), P9(i) and P10(j)

For middle size EG filled foams, the best combination was 730°C casting temperature, 200 bar injection pressure, 30 mm/sec piston speed, 550°C filler pre-temperature and 20 sec piston waiting time. Usually, even though increasing casting temperature affects positively the infiltration ability, some investigators report that between 700-850°C there is a risk of chemical reaction occurring between Al matrix and SiO_2 based filler particles to form hard and brittle Al_2O_3 around the matrix filler interfaces [20]. Atomic diffusion and chemical activities control the kinetics of this reaction while main parameters affecting the extent of the reaction are solidification duration and process temperature. In the fabrication stage, because the all casting processes, regardless of filler size, were carried out at 730 °C with the fast solidification duration (approximately 30 sec), we didn't observe any indications about this chemical activity. Moreover, according to the supplier information, there is a limitation for softening temperature (700°C) of EG spheres, so pre-temperature of the filler particles did not exceed 600°C during the fabrication. In the light of the results for middle size filled foam samples and operation limitations expressed above, both small size and big size EG filled foams were fabricated by optimizing of injection pressure, piston speed, filler pre-temperature and piston waiting time.

As for the fabrication of 0.5-1 mm EG sphere filled foams, injection pressure, piston speed and waiting time were increased up to 210 bar, 40 mm/sec and 30 sec respectively in order to provide effective matrix filtration between very narrow gaps. In addition, EG particles pre-temperature was determined at upper limit of 600°C. However, for 2-4 mm EG sphere filled foams, in comparison with other size groups, the infiltration subject was not a difficult task due to bigger gaps between large size EG spheres as estimated before, hence both injection pressure and piston speed were decreased (170 bar, 20 mm/sec) and only 10 sec waiting time was sufficient for high quality samples. Furthermore, there was no inconvenience for diminishing filler pre-temperature to 500°C. From Fig. 4 given below, all three types of fabricated syntactic foams can be seen.

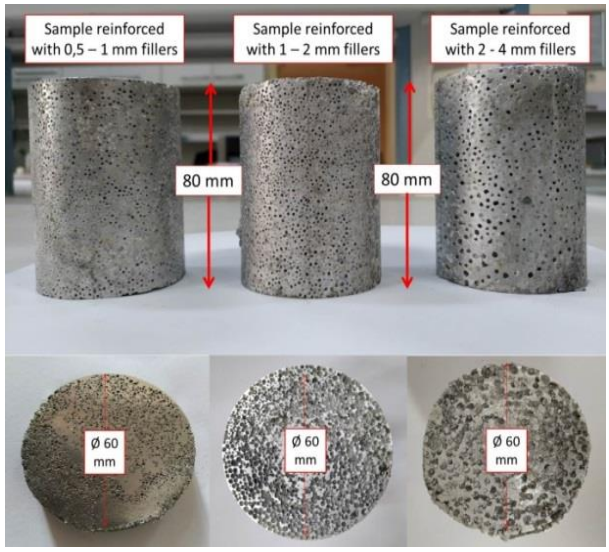

Fig. 4. Fabricated foams and their cross-sectional views

3.2 Microstructural and Physical Properties

After the optimization of the process parameters for each size of EG spheres, fabricated syntactic foams were divided into three groups to examine physical and microstructural features. In this context, these groups were categorized as small EG filled (SF1, SF2 and SF3), medium EG filled (SF4, SF5 and SF6) and big EG filled (SF7, SF8 and SF9).

In the characterization study, microscopic and physical observations were carried out. Before the microscopic examinations, foam samples were cut into two pieces and cross sectional surfaces were grinded with silicon carbide emery papers. Following the grinding, polishing process was applied by using diamond suspension. Also, ultrasonic cleaning was conducted because sample surfaces might possess some unwanted micronized contaminations. With the intention of scrutinizing the microstructure, Nikon Eclipse LV150L and Nikon SMZ800 model microscopes working with DpxView-Pro software were used as well as SEM observations.

Detailed microstructural images of the manufactured foams are shown in Fig. 5 and it is obvious that they are considerably compatible with typical metal syntactic structures stated in previous investigations [4, 13, 21].

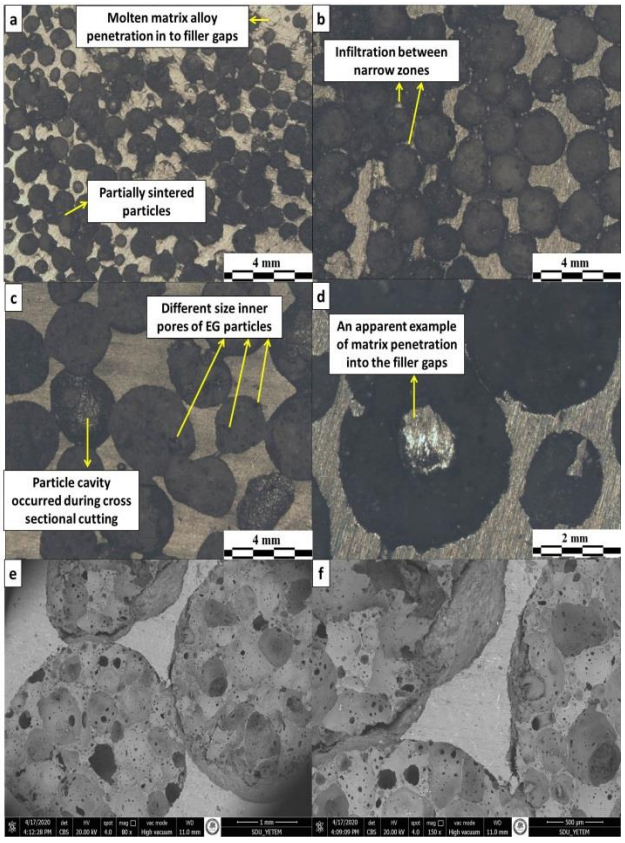

Fig. 5. Optic and SEM images of Al/EG foams: sample with 0.5-1 mm EG (a), sample with 1-2 mm EG (b), sample with 2-4 mm EG (c), matrix penetration (d), partially combining edges (e), narrow line infiltration (f)

It is clear from Fig. 5, all foam samples compose of two primary phases (metallic matrix and porous EG spheres) and certain secondary phases (combined particles, broken sphere fragments and matrix filled spheres). On account of difference in thermal conductivity between the matrix and EG spheres, solidification duration usually alters and exhibit falling tendency from Al/EG interface to the Al matrix itself. This situation sometimes may cause some small casting voids (shrinkage cavities) around the matrix/filler interface. On the other hand, during the manufacturing, due to high pressure and temperature, some EG spheres may combine with each other and behave like bigger size filler (Fig. 5a-c). Besides, in some cases, the liquid Al alloy may penetrate into pores on/into the filler partially or fully depending upon local fractured areas and defective points on the outer surfaces of EG spheres (Fig. 5f). This matrix leakage is a significant circumstance being responsible for the density rising and also affects the mechanical responses and failure characteristics of AMSFs.

As for structural evaluations, volume fraction of Al matrix (F_{alu}), volume fraction of filler particles (F_{fil}) and total porosity percentage (F_{TP}) were determined benefiting some mathematical equations expressed below [7]. In these equations; V_{syn}, m_{syn}, m_{fil}, ρ_{fil}, ρ_{alu} and ρ_{sd} are the syntactic foam volume, the foam mass, the mass of EG spheres, particle density of EG, density of the matrix and density of solid state of the EG spheres respectively.

$$F_{fil} = [(V_{syn}-(m_{syn}-m_{fil})/\rho_{alu})/V_{syn}] \times 100 \quad (1)$$

$$\rho_{fil} = m_{fil}/[V_{syn}-(m_{syn}-m_{fil})/\rho_{alu}] \quad (2)$$

$$F_{TP} = F_{fil} \times [1-(\rho_{fil}/\rho_{sd})] \quad (3)$$

Table 2 drawn below shows major physical features of the all syntactic samples like foam density, volume fraction of the EG spheres and total porosity percentages.

Table 2.
Major physical features of the fabricated foams

Sample No	EG size (mm)	Density (g/cm^3)	EG volume fraction (%)	Total porosity (%)
SF1	0.5-1	1.88	43.5	33.8
SF2	0.5-1	1.84	44.9	35.2
SF3	0.5-1	1.82	45.6	35.9
SF4	1-2	1.96	38.8	30.8
SF5	1-2	1.93	39.9	31.9
SF6	1-2	1.89	41.3	33.3
SF7	2-4	2.06	34.5	27.2
SF8	2-4	2.02	36.0	28.6
SF9	2-4	2.01	36.3	28.9

From the Table 2, syntactic foam density values range between 1.82 and 2.06 g/cm^3 with the average of 1.93 g/cm^3. EG spheres utilized in this investigation have thin walled outer surface and porous inner structure, so total foam porosity depends to porosity levels of EG spheres on a large scale. Herein, the outcomes indicate that small size EG filled SF3 has the highest porosity level with %35.9 whereas big size EG filled SF7 possess the lowest value of %27.2. Furthermore, there is a positive relation between total foam porosity values and volume fractions of EG spheres. As a consequence of the volumetric calculations, maximum EG volume fraction of %45.6 is obtained for SF3 having the highest porosity level although minimum EG volume fraction of 34.5 belongs to SF7 having the lowest porosity level. If the size range of EG spheres takes into consideration, it can be asserted that as long as the size of EG spheres increases syntactic foam density and total porosity values also rise directly (Fig. 6). This case can attribute to the fact that small spheres have higher compaction and packing factors compared to middle and big spheres.

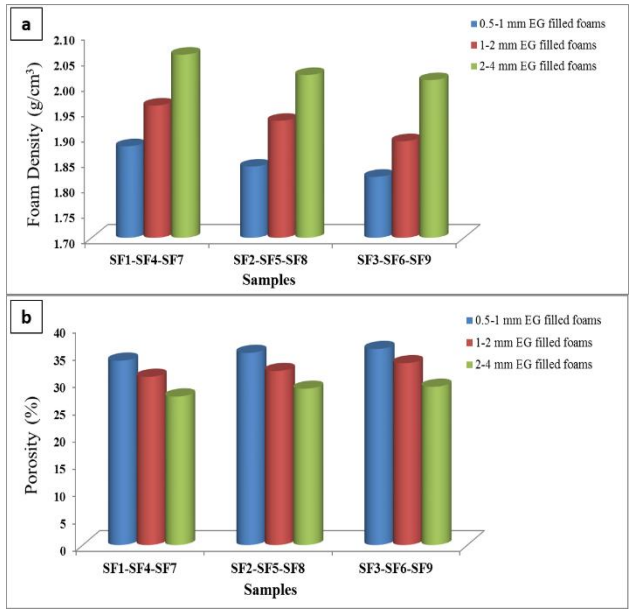

Fig. 6. Relationships between EG particle size and foam density (a) and total porosity (b)

3.3 Relations between Injection Parameters and Physical Features

In the optimization works, as estimated before, it was observed that as the size of EG particles became smaller, injection pressure and piston speed went up from 170 bar to 210 bar and from 20 mm/sec to 40 mm/sec respectively. This was a result of lesser volume (lesser narrow gaps) occupied by big size particles in the die cavity in which the molten Al alloy filled. Likewise, pre-temperature of EG spheres and piston waiting time displayed upward tendency depending on decreasing particle size by reason of difficult infiltration and early solidification danger of the Al matrix. As regards to the casting temperature, there was no an apparent difference between each size groups and it was determined as 720°C for 2-4 mm EG filled foams and as 730°C for both 0.5-1 mm and 1-2 mm EG filled foam. From Fig. 7, the relationship between EG particle size and the cold chamber die casting process parameters can be understood clearly.

On the purpose of understanding the effects of injection factors on the density values of the syntactic foams, some extra

samples having 2-4 mm EG spheres were manufactured by not changing optimum process levels except for analyzed parameters.

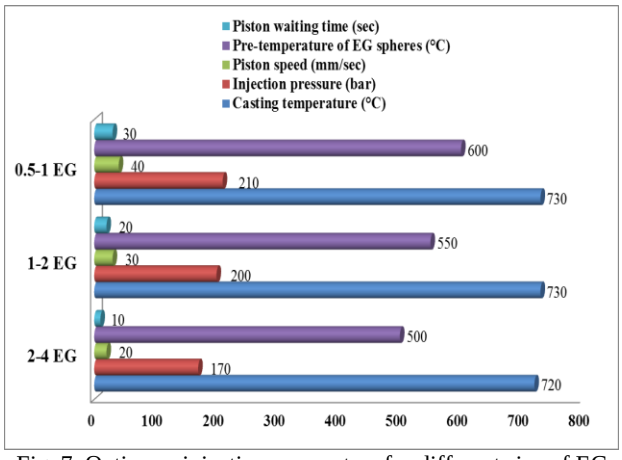

Fig. 7. Optimum injection parameters for different size of EG spheres

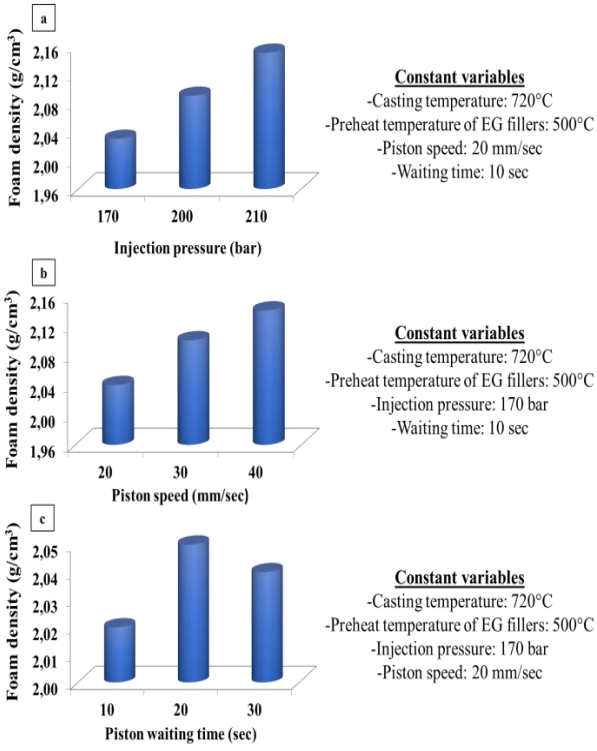

Fig. 8. Relation between injection parameters and foam density: injection pressure (a), piston speed (b) and waiting time (c)

According to the analysis of physical properties of the fabricated foams depicted in Fig. 8, injection pressure and piston speed are the most influential parameters in terms of the foam density. Thanks to high injection pressure and rapid piston movement, diminishing gas solubility as much as possible and closing majority of infiltration gaps are accomplishable. Therefore, in the fabrication, as a consequence of being minimized casting voids and gas solubility, it is correct to say that the more injection pressure and piston speed are applied, the higher foam density or the lower foam porosity can be attained. Compared to injection pressure and piston speed, despite of the fact that piston waiting time is an effective variable for fabrication of different size EG filled Al foams, its role, which results in rising tendency, on the foam density can be assessed as minor.

Together with the high injection pressure and piston speed, probability of filler breakage which is definitely undesirable for AMSFs, increases due to excessive amount of liquid aluminum metal penetration into the EG spheres. It is also well known that characteristic mechanical properties (compression strength, plateau strength, energy absorption capacity, elongation till the densification point and energy absorption efficiency) and fracture behaviors of these advanced foams depends strongly their densities and porosity values. Although higher density levels mean better yield strength due to increment of the volume fraction of load bearing metal matrix material, they result in lower specific strength and worse energy absorption ability because of decreasing total porosity. In this point, as it is also tried in this paper, process optimization works are notably crucial for fabricating quality products having homogenous and minimum defective inner structures.

4. Conclusions

As a result of this experimental investigation on metal matrix syntactic composite foams, the following conclusion remarks can be listed:

- Al 7075/EG syntactic foams can be fabricated effectively by industrial focused high pressure cold chamber die casting method which is clearly superior in terms of real industrial applications than previously reported laboratory scaled techniques. In the near future, by means of this industrial focused process, larger and complex shaped metal matrix syntactic foams can be produced in a short process durations without any setbacks,
- As long as the EG sphere size shrinks, measured density values of the fabricated foams diminish in a noteworthy manner. While the minimum density of 1.82 g/cm^3 belongs to small sized 0.5-1 mm EG filled sample of SF3, 2-4 mm EG filled big sized sample of SF7 has the highest density value with 2.06 g/cm^3,
- Total porosity values of the produced foams largely depend on the EG sphere size and it is evident that there is a negative relation between them. 0.5-1 mm EG filled sample of SF3 possesses the highest porosity value of %45.6,
- As the EG sphere size becomes bigger, infiltration of the Al matrix between EG particles gets easier and required injection pressure, piston speed, piston waiting time, pre-temperature of the EG spheres and casting temperature values decrease due to wide penetration gaps,
- In the fabrication of high quality foams having homogenous inner structures, in order to minimize damaging of EG spheres, to block undesired chemical reactions and to avoid

density rising, correct optimization of casting parameters is highly important,

– Injection pressure and piston speed are the most decisive factors on the physical properties of the fabricated Al syntactic foams. If these parameters go up in accordance with the cold chamber die casting machine capacity, it is seen that density values of the foams also increase up to 2.14 g/cm^3 due to decreasing inner porosity.

Acknowledgements

This article was supported by The Scientific and Technological Research Council of Turkey (TÜBİTAK) with the project ID of 116M533. We also would like to thank to Omnis Composite Limited Company for rapid supplying of high quality EG spheres.

References

[1] Licitra, L., Luong, D.D., Strbik III, O.M. & Gupta, N. (2015). Dynamic properties of alumina hollow particle filled aluminum alloy A356 matrix syntactic foams. *Materials and Design*. 66(B), 504-515. DOI: 10.1016/j.matdes. 2014.03.041.

[2] Taherishargh, M., Belova, I.V., Murch, G.E. & Fiedler, T. (2015). Pumice/aluminum syntactic foam. *Materials Science & Engineering* A. 635, 102-108. DOI: 10.1016/j.msea.2015.03.061.

[3] Szlancsik, A., Katona, B., Májlinger, K. & Orbulov, I.N. (2015). Compressive behavior and microstructural characteristics of iron hollow sphere filled aluminum matrix syntactic foams. *Materials*. 8(11), 7926-7937. DOI: 10.3390/ma8115432.

[4] Mondal, D.P., Das, S., Ramakrishnan, N., & Uday Bhasker, K. (2009). Cenosphere filled aluminum syntactic foam made through stir-casting technique, *Composites: Part A*. 40(3), 279-288. DOI: 10.1016/j.compositesa.2008.12.006.

[5] Lin, Y., Zhang , Q., Ma, X. & Wu, G. (2016). Mechanical behavior of pure Al and Al–Mg syntactic foam composites containing glass cenospheres. *Composites: Part A*. 87, 194-202. DOI: 10.1016/j.compositesa.2016.05.001.

[6] Orbulov, I.N. & Dobránszky, J. (2008). Producing metal matrix syntactic foams by pressure infiltration. *Periodica Polytechnica Mechanical Engineering*. 52(1), 35-42. DOI: 10.3311/pp.me.2008-1.06.

[7] Taherishargh, M., Belova, I.V., Murch, G.E. & Fiedler, T. (2014). Low-density expanded perlite–aluminium syntactic foam. *Materials Science & Engineering* A. 604, 127-134. DOI: 10.1016/j.msea.2014.03.003.

[8] Al-Sahlani, K., Broxtermann, S., Lell, D. & Fiedler, T. (2018). Effects of particle size on the microstructure and mechanical properties of expanded glass-metal syntactic foams. *Materials Science and Engineering* A. 728, 80-87. DOI: 10.1016/j.msea.2018.04.103.

[9] Dolata-Grosz, A., Dyzia, M. & Śleziona, J. (2008). Structure and technological properties of AlSi12 –(SiCp + Cgp) composites. *Archives of Foundry Engineering*. 8(1), 43-46.

[10] Cholewa, M. & Kondracki, M. (2010). Cast composites with Al-matrix reinforced with intermetallic carbide phases. *Archives of Foundry Engineering*. 10(4), 95-99.

[11] Niranjan, K. & Lakshminarayanan, P.R. (2013). Optimization of process parameters for in situ casting of Al/TiB2 composites through response surface methodology. *Transactions of Nonferrous Metals Society of China*. 23(5), 1269-1274. DOI: 10.1016/S1003-6326(13)62592-3.

[12] Zhang, Q., Lee, P.D., Singh, R., Wu, G. & Lindley, T.C. (2009). Micro-CT characterization of structural features and deformation behavior of fly ash/aluminum syntactic foam. *Acta Materialia*. 57(10), 3003-3011. DOI: 10.1016/j.actamat.2009.02.048.

[13] Tao, X.F., Zhang, L.P. & Zhao, Y.Y. (2009). Al matrix syntactic foam fabricated with bimodal ceramic microspheres. *Materials & Design*. 30(7), 2732-2736. DOI: 10.1016/j.matdes.2008.11.005.

[14] Orbulov, I.N. (2013). Metal matrix syntactic foams produced by pressure infiltration-The effect of infiltration parameters. *Materials Science & Engineering* A. 583, 11-19. DOI: 10.1016/j.msea.2013.06.066.

[15] Katona, B., Szlancsik, A., Tábic, T. & Orbulov, I.N. (2019). Compressive characteristics and low frequency damping of aluminum matrix syntactic foams. *Materials Science & Engineering* A. 739, 140-148. DOI: 10.1016/j.msea.2018.10.014.

[16] Goel, M.D., Parameswaran, V. & Mondal, D.P. (2019). High strain rate response of cenosphere-filled aluminum alloy syntactic foam. *Journal of Materials Engineering and Performance*. 28, 4731-4739. DOI: 10.1007/s11665-019-04237-2.

[17] Mondal, D.P., Goel, M.D., Upadhyay, V., Das, S., Singh, M. & Barnwal, A.K. (2018). Comparative study on microstructural characteristics and compression deformation behaviour of alumina and cenosphere reinforced aluminum syntactic foam made through stir casting technique. *Transactions of the Indian Institute of Metals*. 71, 567-577. DOI: 10.1007/s12666-017-1211-x.

[18] Vishwakarma, A., Mondal, D.P., Birla, S., Das, S. & Prasanth N. (2017). Effect of cenosphere size on the dry sliding wear behaviour LM13-cenosphere syntactic foam. *Tribology International*. 110, 8-22. DOI: 10.1016/j.triboint.2017.01.041.

[19] Akinwekomi, A.D., Adebisi, J.A. & Adediran, A.A. (2019). Compressive characteristics of aluminum-fly ash syntactic foams processed by microwave sintering. *Metallurgical and Materials Transactions* A. 50, 4257-4260. DOI: 10.1007/s11661-019-05347-1.

[20] Balch, D.K. & Dunand, D.C. (2006). Load partitioning in aluminum syntactic foams containing ceramic microspheres. *Acta Materialia*. 54(6), 1501-1511. DOI: 10.1016/j.actamat.2005.11.017.

[21] Gupta, N., Luong, D.D. & Cho, K. (2012). Magnesium matrix composite foams—Density, mechanical properties and applications. *Metals*. 2, 238-252. DOI: 10.3390/met2030238.